Improved Charge Carrier Transport of Hydrogen-Treated Copper Tungstate: Photoelectrochemical and Computational Study

Wenlong Guo,[a,b] **Zhiyao Duan,**[c] **Oluwaniyi Mabayoje,**[d] **William D. Chemelewski,**[e] **Peng Xiao,**[f] **Graeme Henkelman,**[c] **Yunhuai Zhang,**[b,z] **and C. Buddie Mullins**[a,d,e,*,z]

[a]*McKetta Department of Chemical Engineering, University of Texas at Austin, Austin, Texas 78712-0231, USA*
[b]*College of Chemistry and Chemical Engineering, Chongqing University, Chongqing 400030, People's Republic of China*
[c]*Department of Chemistry and the Institute for Computational Engineering and Sciences, The University of Texas at Austin, Austin, Texas 78712-0165, USA*
[d]*Department of Chemistry and Biochemistry, Center for Electrochemistry, and Center for Nano- and Molecular Science, University of Texas at Austin, Austin, Texas 78712-0231, USA*
[e]*Texas Materials Institute, University of Texas at Austin, Austin, Texas 78712-0231, USA*
[f]*College of Physics, Chongqing University, Chongqing, 400030, People's Republic of China*

Thin films of copper tungstate ($CuWO_4$) have been prepared through electrodeposition and tested as the anode material for photoelectrochemical (PEC) water oxidation. We found that hydrogen-treatment over the synthesized $CuWO_4$ at high temperatures led to enhancement in the PEC performance for water oxidation. The origin of this activity enhancement is attributed to the enhanced kinetics of electron-hole pair separation due to the increased carrier concentration induced by oxygen vacancy formation upon hydrogen-treatment. The incorporation of oxygen vacancies also resulted in enhanced light absorbance in the visible light region because they introduce shallow donors as predicted by first-principles calculations. Nevertheless, incident photon to electron conversion efficiency (IPCE) measurements indicate that light absorbed at long wavelength region after hydrogen-treatment is not successfully utilized to oxidize water. This report provides insights on the effect of hydrogen-treatment on the structural, optical, and electronic properties of $CuWO_4$.

Solar energy is a sustainable and abundant energy source which has the potential to alleviate energy and environmental issues caused by the large-scale consumption of fossil fuels and also to simultaneously fulfill the ever-increasing energy demand of mankind.[1] Among a variety of fuels that can be produced by artificial photosynthesis, solar production of hydrogen from protons through photoelectrochemical (PEC) water splitting stands out and provides a viable, clean, low cost, and renewable energy source.[2,3] Stimulated by the possibility of using hydrogen from water as a source of energy, a significant amount of research has been devoted to searching for efficient semiconductor materials as electrodes for the PEC water splitting since the pioneering work of Fujishima and Honda on n-type TiO_2 photoelectrodes in 1972.[4] Despite continuous efforts over decades, the search for a suitable electrode that could lead to the practical application of PEC water splitting for hydrogen production has so far failed due to the harsh and even contradictory requirements an ideal electrode should meet, such as sufficient bandgap, proper band edge positions, ability to utilize visible light, low rate of electron-hole recombination, suppression of reverse reactions, insolubility in water, and high corrosion resistance, to name a few. TiO_2 suffers from the inability to harness visible light due to its large bandgap (3–3.2 eV).[5,6] α-Fe_2O_3 has a suitable bandgap of 2.1 eV, but it suffers from low charge carrier mobility and a short hole diffusion length.[7,8] WO_3 is soluble in water at pH greater than 5 and can only absorb the blue-violet part of visible light spectrum because of its large bandgap of 2.7 eV.[9,10]

These deficiencies of binary metal oxides drive attention to ternary oxides since the properties of binary oxides could be modulated by the addition of a new element. To circumvent the drawbacks of WO_3, triclinic copper tungstate ($CuWO_4$) has attracted much attention.[11–20] $CuWO_4$ has a direct bandgap of $\sim$2.4 eV. The narrowed bandgap, as compared to WO_3, was explained by the raised valence band maximum due to the hybridization of Cu(3d) and O(2p) orbitals.[15,21] $CuWO_4$ also has improved stability in neutral electrolyte compared to WO_3.[22] This advantage can also be traced to the strong Cu-O bond, which limits the formation of soluble tungstate. However, the introduction of localized Cu(3d) orbitals also lead to poor charge transport properties.[21] Therefore, enhancing the mobility of charge carriers in

$CuWO_4$ is a crucial step to improve its PEC performance. A number of strategies have been tried to address this limitation. Most recently, Zhang et al. reported that the photocurrent density of $CuWO_4$ is significantly increased by the incorporation of Ag nanowires into the semiconductor matrix, which enhances the conductivity of $CuWO_4$.[23] Bohra et al. found that the charge separation efficiency of $CuWO_4$ can be increased by doping Fe, which results in an improved solar-to-hydrogen conversion efficiency.[24]

Hydrogen-treatment can reduce metal oxide semiconductor materials by introducing oxygen vacancies and hydrogen impurities and thus is a simple method to increase the donor density and electrical conductivity. In recent years, several common photoanodes, TiO_2,[25–30] α-Fe_2O_3,[31,32] WO_3,[33] and $BiVO_4$,[34,35] have been treated using this method and resulted in photocurrent density enhancement. By analogy, in this work, the annealed electrodeposited $CuWO_4$ films were further thermally treated under an atmosphere of 5% hydrogen in argon. We observed an enhancement of light absorbance in the visible light range and an increase in photocurrent density after hydrogen-treatment. By combining experimental and theoretical methods, we discovered that the mid-gap states generated by O vacancies are responsible for the stronger absorption of visible light. However, the enhanced absorbed visible light is not utilized for water oxidation as shown by IPCE measurements. The increased photocurrent density can therefore be explained by the enhanced charge carrier density as evidenced by Mott-Schottky measurements.

Results and Discussion

Material characterization.—Figure 1 shows the morphologies of the annealed $CuWO_4$ film and hydrogen-treated $CuWO_4$ film prepared at 250°C (this sample shows the highest photocurrent density). For simplicity, we use H_2:$CuWO_4$ to denote the hydrogen-treated $CuWO_4$ sample with optimal performance in the following discussions. The SEM images reveal that the electrodeposited $CuWO_4$ films are porous and could be described as interconnected nanoparticles. The particle size distributions based on SEM images are measured using ImageJ software[36] and there is no obvious difference in the average particle sizes before and after hydrogen-treatment ($\sim$200 ± 10 nm). The thickness of the $CuWO_4$ film is about 2.5 μm observed from the cross sectional SEM image (shown in Figure S3). The stoichiometry of the

*Electrochemical Society Member.
[z]E-mail: mullins@che.utexas.edu; xp2031@163.com
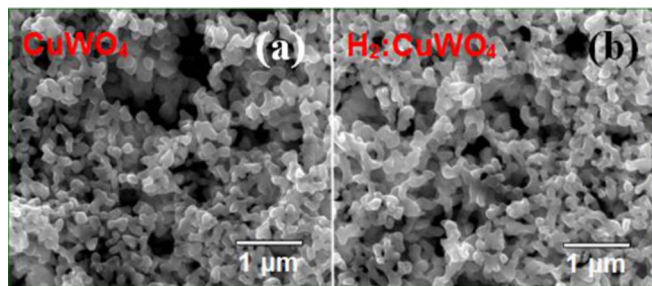
Figure 1. Top view of SEM images for the (a) CuWO$_4$ and (b) H$_2$:CuWO$_4$ films.

film was checked with eight individually synthesized samples. The value of Cu/W ratio is close to the formal composition of 1.0 for CuWO$_4$ (shown in Figure S4).

The synthesized thin film was further characterized by XRD to determine the phase of the materials and the effect of hydrogen-treatment on the material's crystallinity. As shown in Figure 2a, XRD patterns of annealed CuWO$_4$ films can only be indexed to triclinic CuWO$_4$ (PDF # 01-088-0269). After hydrogen-treatment at various temperatures, the XRD spectrum of the CuWO$_4$ thin film remains unchanged, indicating that hydrogen-treatment did not change the degree of crystallinity and the phase of the material. When the XRD patterns are examined more closely for 2θ values at 17–21°, 22–25°, and 30.5–33°, as respectively shown in Figures 2b, 2c, and 2d, noticeable shifts of diffraction peaks after hydrogen-treatment are observed. The center position of the (100) peak shifts from 18.98° (the center of the (100) peak for CuWO$_4$) to 19.03° (the center of the (100) peak for CuWO$_{4-x}$ (PDF # 00–021–0307)). The (0$\bar{1}$0), (011), and (020) peaks centered at 23.54°, 23.58°, and 30.82° for CuWO$_4$ also shift to 24.10°, 24.16°, and 30.86°, respectively. All these shifts

are consistent with the formation of CuWO$_{4-x}$. Hence, it is suggested that oxygen vacancies have been introduced into the lattice of CuWO$_4$ by hydrogen-treatment.

X-ray photoelectron spectroscopy (XPS) measurements were conducted to characterize the chemical states of CuWO$_4$ and H$_2$:CuWO$_4$ films. The position of adventitious carbon C 1s peak is assigned to 284.8 eV to calibrate the binding energy scale.

Figure 3a shows that the Cu(2p$_{1/2}$) and Cu(2p$_{3/2}$) peaks of CuWO$_4$ are located at binding energies of 954.51 and 934.52 eV, respectively, which are in good agreement with the reported values for CuWO$_4$.[15] For H$_2$:CuWO$_4$, both Cu(2p$_{1/2}$) and Cu(2p$_{3/2}$) lines shift slightly to the low binding energies by 0.34 and 0.31 eV to 954.17 and 934.21 eV, respectively. According to the literature,[37,38] these shifts are due to the partial reduction of Cu^{2+} species. The core-level W 4f XPS spectra of the CuWO$_4$ and H$_2$:CuWO$_4$ films are shown in Figure 3b. The shift of binding energies to the low binding energy for W(4f$_{5/2}$) and W(4f$_{7/2}$) peaks is 0.28 and 0.27 eV upon hydrogen-treatment, respectively. This result suggests the existence of W^{5+} species, which have been demonstrated to have lower binding energies of 4f$_{5/2}$ and 4f$_{7/2}$ electrons than those of the W^{6+}.[33] As shown in Figure S5, O 1s XPS spectra of CuWO$_4$ consist of two peaks centered at 530.10 and 531.01 eV. The peak at 530.10 eV is consistent with the typical binding energy of the O(1s) line of CuWO$_4$, while the peak at 531.01 eV can be assigned to surface hydroxide.[15] The second peak shifts from 531.01 eV to 531.32 eV. A similar behavior has been observed for hydrogen treated BiVO$_4$.[35] XPS analysis shows that the metal components of CuWO$_4$ are partially reduced after hydrogen-treatment due to oxygen vacancies, which is in agreement with the result from XRD.

Optical and electrical properties.—As shown in Figure S2, the incorporation of oxygen vacancies into the CuWO$_4$ thin film leads to dramatic color change of the samples. The sample color becomes visibly darker after hydrogen-treatment. This apparent darkening becomes more obvious for samples annealed at higher temperatures. The
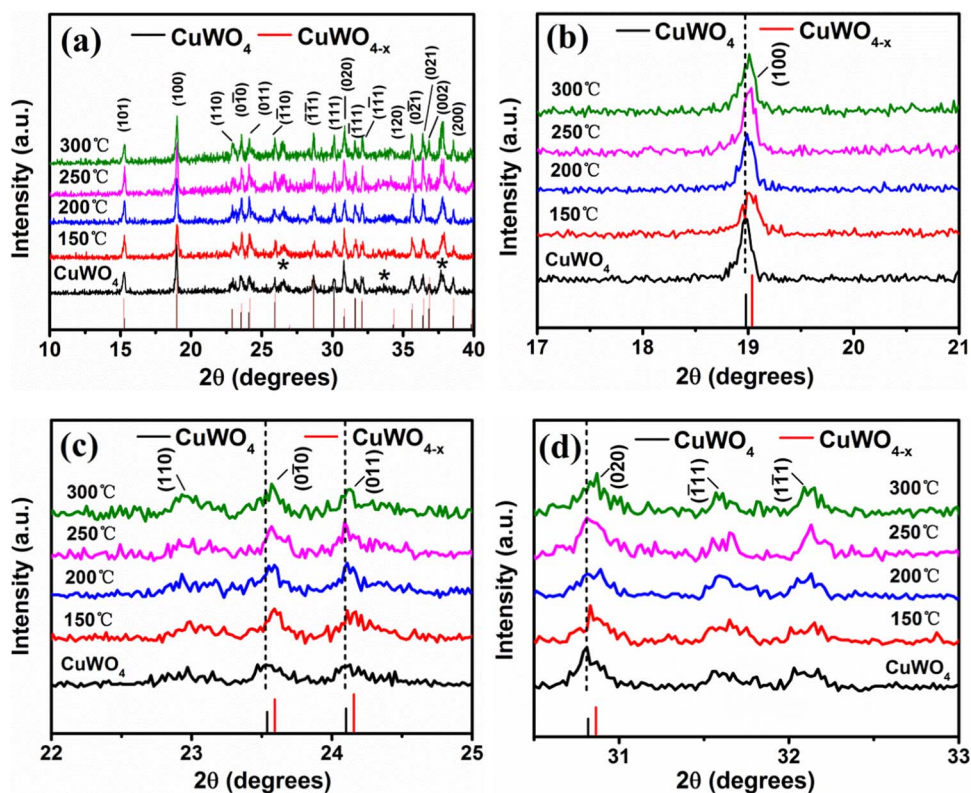
Figure 2. (a) XRD patterns of the CuWO$_4$ and hydrogen-treated CuWO$_4$ films (treated at various temperatures). The black and red vertical lines correspond to CuWO$_4$ (PDF# 01-088-0269) and CuWO$_{4-x}$ (PDF# 00-021-0307), respectively. The * symbols indicate the peaks for SnO$_2$ (PDF# 00-046-1088). (b), (c), and (d) enlarged portion of XRD patterns for 2θ values 17–21°, 22–25°, and 30.5-33°, respectively.
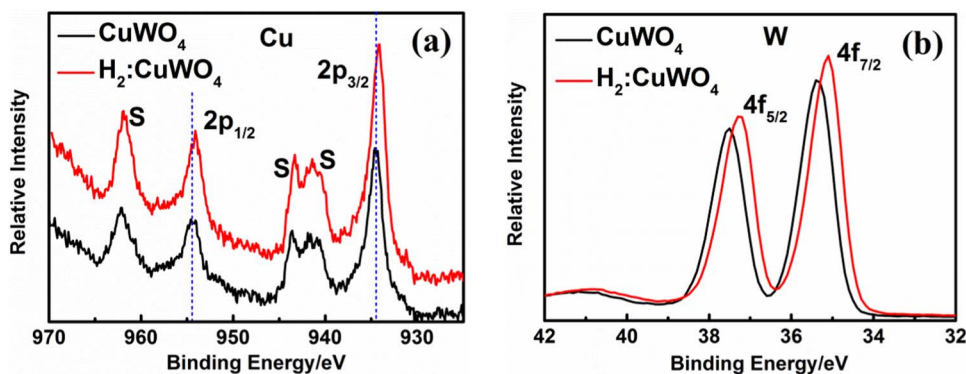
Figure 3. XPS spectra of the (a) Cu 2p and (b) W 4f peaks for the CuWO$_4$ and H$_2$:CuWO$_4$ films. The S symbols in (a) indicate the satellite peaks.

color change indicates the change of the optical properties of CuWO$_4$. The influence of the hydrogen-treatment on the optical properties of CuWO$_4$ was probed by UV-vis absorbance. The light absorption of H$_2$:CuWO$_4$ almost increases over the entire tested wave length region except from 350 to 375 nm (Figure 4). An increased UV-vis absorption has been previously observed in other hydrogen-treated metal oxides, notably TiO$_2$.[8,25] The authors have ascribed this increase to the introduction of oxygen vacancies and the increased hydroxyl groups that act as visible light-active defect sites. The net result is a broad increase in absorption of visible light to and from the mid-bandgap energy states of these defect sites, which results in the change from white to black TiO$_2$ coloration. The hydrogen treatment of our CuWO$_4$ films creates similar vacancies which likewise act to increase film absorption. In addition to the optical properties, electrical properties are also shifted after hydrogen-treatment.

Figure 5 presents the Mott-Schottky plots measured in 0.1 M KBi buffer at the frequency of 5 kHz. Linear regression of the $1/C^2$ vs V relationship gives an estimated flatband potential of ~0.48 V and ~0.52 V vs RHE for CuWO$_4$ and H$_2$:CuWO$_4$, respectively. The positive slopes of the regression lines indicate the n-type semiconductor properties of CuWO$_4$ and H$_2$:CuWO$_4$. According to the literature,[39] the charge carrier densities of these films at 5 kHz frequency can be calculated (a dielectric constant of 83 for CuWO$_4$ is used[11]). The charge carrier density of the pristine CuWO$_4$ film is calculated to be 3.08×10^{18} cm^{-3}, while the calculated charge carrier density of the H$_2$:CuWO$_4$ film is 7.42×10^{18} cm^{-3} - more than twice that found for the untreated CuWO$_4$ film.

Electronic structure by first-principles calculations.—The density of states (DOS) plot of CuWO$_4$ from a DFT-HSE06 calculation is shown in Figure 6a. The bandgap is calculated to be 2.4 eV, which is in agreement with experiments.[14,15,17] The valence band bottom

mainly consists of W(5d) states, while the Cu(3d) states contribute primarily to the middle part of the valence band. O(2p) states contribute substantially to the whole valence band region and especially to the top of the valence band. The conduction band can be clearly divided into two sub-bands. Cu-O hybridized states are the principal contributor to the sub-band at lower energy from 2.4 eV to 3.8 eV above the valence band. The upper conduction band mainly originates from the W-O interaction above 3.8 eV. The absorption spectrum (the imaginary part of the dielectric function) is shown in Figure 6c. The first peak is a resonant excitonic peak located at 2.1 eV. It corresponds to the optical bandgap of 2.2 eV and matches very well with the yellowish color of CuWO$_4$. There are two other small peaks located at 3.2 eV and 3.6 eV, respectively. The third peak at 3.6 eV corresponds to the direct quasiparticle bandgap obtained with the G0W0 method. The energy difference between the first and third peak gives an exciton binding energy of 1.5 eV. The major peak centered at 4.5 eV originates from the excitation from the valence band top to the higher part of the conduction band consisting of mainly W(5d) and O(2p) states.

Upon the generation of oxygen vacancies, Cu and W atoms are reduced. The Bader charges of Cu atoms shift from 9.66e to 10.06e, while the Bader charges of W change from 10.84e to 11.03e. The magnetic moments of Cu atoms also reduce to zero. The DOS changes dramatically as shown in Figure 6b. It can be seen that occupied mid-gap states corresponding to the Cu(3d) states are introduced into the DOS lying approximately 0.8 eV below the W(3d)-O(2p) conduction band. As a result, O vacancies can induce shallow donors into the CuWO$_4$ band structures. This is in agreement with the result obtained from Mott-Schottky plots, in which it is shown that the
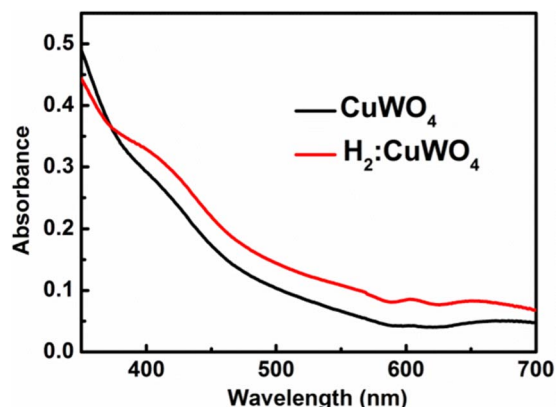
Figure 4. UV-vis absorbance of the CuWO$_4$ and H$_2$:CuWO$_4$ films.
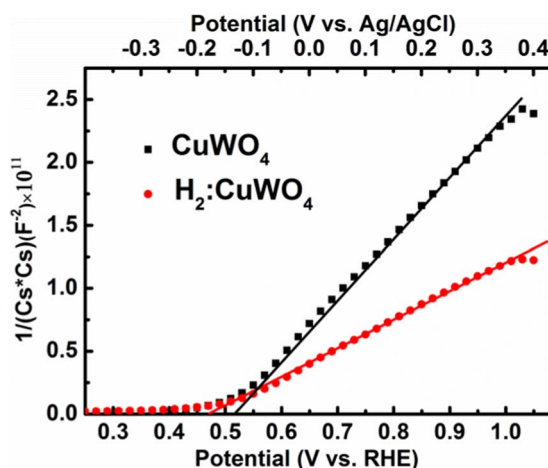
Figure 5. Mott-Schottky plots of the CuWO$_4$ and H$_2$:CuWO$_4$ films obtained in 0.1 M KBi buffer solution (pH 7.0) at the frequency of 5 kHz.
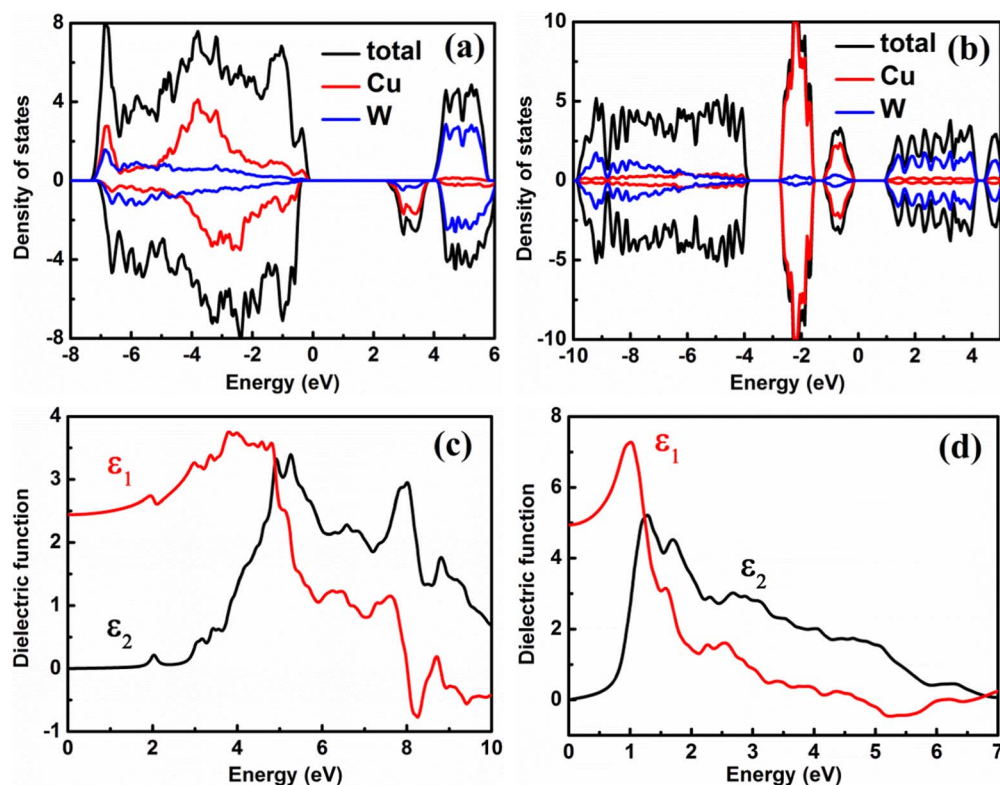
Figure 6. Computed total and partial density of states of (a) $CuWO_4$ and (b) $CuWO_4$ with O vacancies. Computed absorption spectra (imaginary part of dielectric function) of (c) $CuWO_4$ and (d) $CuWO_4$ with O vacancies.

charge carrier density of the $CuWO_4$ film is increased by hydrogen-treatment. Consistent with the electronic structure, the absorption spectrum of $CuWO_4$ with O vacancies (shown in Figure 6d) exhibits much higher absorption in the low energy regime than untreated $CuWO_4$. This computational result is also consistent with observations from UV-vis absorption spectra. Light absorption in the long wave-length region can be attributed to the transitions from the valence band of $CuWO_4$ to the oxygen vacancy level or from the oxygen vacancy level to the conduction band of $CuWO_4$.[26,28]

PEC measurements.—The PEC properties of the pristine $CuWO_4$ and hydrogen-treated $CuWO_4$ films were measured with linear sweep voltammetry (LSV) experiments. In these measurements, we used a 0.1 M KBi buffer solution of pH = 7.0 as the electrolyte because $CuWO_4$ shows high O_2 evolution faradaic efficiency ($\sim$97%) and only slight degradation in this solution.[22] Results of these measurements are shown in Figure 7a. It can be seen that $CuWO_4$ films exhibit higher photocurrent density after hydrogen-treatment. Particularly, the $CuWO_4$ film treated at 250°C showed the highest photocurrent density at 1.23 V vs. RHE, which is about 50% higher in efficiency compared with the non-treated film.

From the discussions of the last section, the incorporated O vacancies can introduce shallow donors into the bandgap, which result in an increase in charge carrier density and enhanced visible light absorption. The improved activity observed in the PEC experiments should be related to the two effects induced by O vacancies. In one way, the increased charge density could result in the enhancement of the strength of electric field in the depletion layer, which then leads
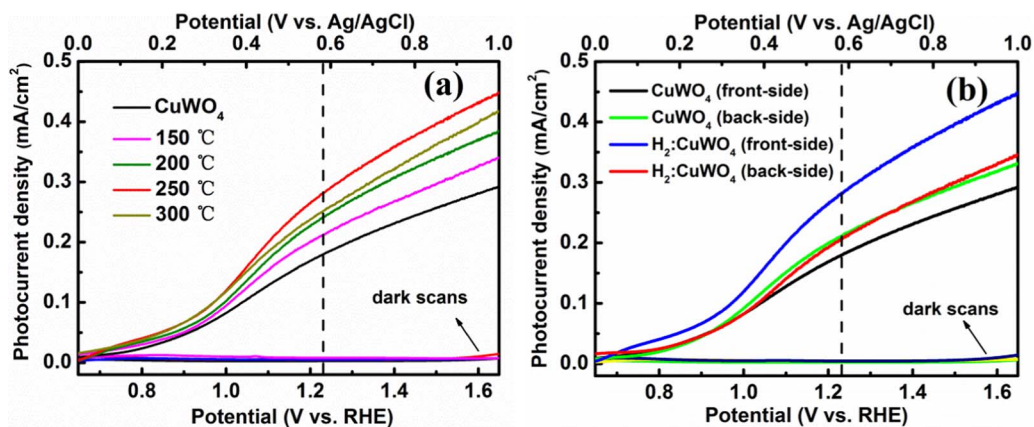
Figure 7. (a) LSV of the $CuWO_4$ and hydrogen-treated $CuWO_4$ films (treated at various temperatures for 20 min) from the front-side illumination in 0.1 M KBi buffer solution (pH 7.0) under AM1.5G simulated solar light (100 mW/cm^2). (b) LSV of the $CuWO_4$ and H_2:$CuWO_4$ films from the front-side and back-side illumination in 0.1 M KBi buffer solution (pH 7.0) under AM1.5G simulated solar light (100 mW/cm^2). The scan rate was 25 mV/s.
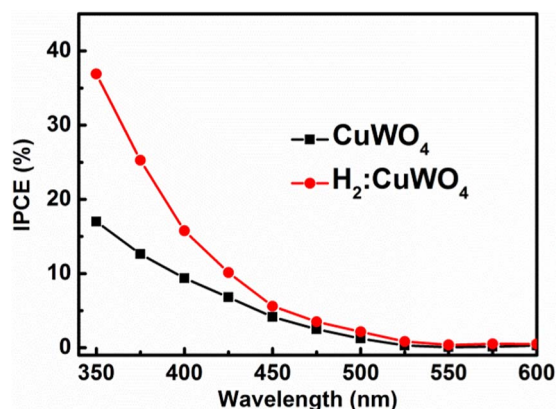
Figure 8. IPCE vs wavelength taken at 1.23 V vs RHE for the $CuWO_4$ and H_2:$CuWO_4$ films under front-side illumination.

to faster electron-hole pair separation. In the other way, the increased numbers of electron-hole pairs generated by the absorption of visible light could directly participate into the reaction.

To examine the idea of enhanced electron-hole pair separation kinetics, we examined the influence of illumination direction on PEC activity. During the PEC measurements, two illumination directions – front-side and back-side – are included. The front-side is the interface of $CuWO_4$ thin film and electrolyte, while the back-side is at the interface of $CuWO_4$ thin film and the FTO electrode. For electron-hole pairs generated at the front-side, photoelectrons need to travel across the whole thickness of thin film to get to the FTO electrode. On the other hand, a photo-electron generated at the back-side is in the vicinity of the FTO electrode. As shown in Figure 7b, the photocurrent of the non-treated $CuWO_4$ film from back-side illumination ($\sim$0.21 mA/cm^2) is higher than that of front-side illumination ($\sim$0.16 mA/cm^2) at 1.23 V vs RHE. The reason for the difference relates to the diffusion length the excited electron needs to travel to the FTO and hole collection depends only on the size of the nanoparticle due to the porous morphology. However, the trend reverses after hydrogen-treatment. The photocurrent of H_2:$CuWO_4$ with front-side illumination ($\sim$0.26 mA/cm^2) is higher than that of back-side illumination ($\sim$0.20 mA/cm^2), which indicates that the electron diffusion is greatly enhanced so that it is no longer limits the photocurrent. An increase in the electron diffusion length in hydrogen-treated $CuWO_4$ does not have an obvious effect on the photocurrents under back-side illumination. This is because for the back-side illuminated samples the electron diffusion length in pristine $CuWO_4$ is already appropriate for the transfer of photogenerated electrons to the FTO substrate. Therefore the photocurrents under back-side illumination for $CuWO_4$ and H_2:$CuWO_4$ are quite similar.

To test the second hypothesis for activity enhancement, the IPCE measurements were performed to investigate the relation between the wavelength of the incident light and the PEC activity. Figure 8 shows the IPCE spectra for $CuWO_4$ and H_2:$CuWO_4$ films at 1.23 V vs RHE. For both $CuWO_4$ and H_2:$CuWO_4$, a photoresponse is observed from 350 to 525 nm. However, the IPCE of H_2:$CuWO_4$ does not increase for wavelengths larger than 525 nm, just as with untreated $CuWO_4$. These results imply that light absorbed at wavelengths of greater than 525 nm is not successfully used to carry out water oxidation. Similar phenomenon has also been observed for hydrogen-treated TiO_2.[26,28] These authors attributed this to the inefficient collection of charge carriers generated with long wavelength light excitation because of their overall short lifetime.

A stability test for 3600 s was made to measure the photostability of $CuWO_4$ and H_2:$CuWO_4$ photoanodes. The photoelectrochemical stability of the $CuWO_4$ and H_2:$CuWO_4$ films from front-side illumination under a constant bias of 1.23 V vs RHE is shown in Figure S6. For $CuWO_4$, the photocurrent approaches a stable anodic current of $\sim$0.17 mA/cm^2 after a slight decrease during the first few minutes

and decreases $\sim$2% of photocurrent over 3600 s showing an excellent stability in 0.1 M KBi buffer (pH 7.0). For H_2:$CuWO_4$, a decrease of $\sim$9% in the photocurrent is observed after 3600 s test. This indicates that the hydrogen-treated $CuWO_4$ films have an acceptable photostability although they are not as stable as the untreated $CuWO_4$ films.

Conclusions

In summary, it has been shown that hydrogen-treatment of $CuWO_4$ leads to an enhanced PEC activity in water oxidation. The XRD and XPS analysis of pristine and hydrogen-treated $CuWO_4$ show that the improved activity due to hydrogen-treatment is due to the formation of oxygen vacancies. In addition, the formation of oxygen vacancies results in a higher carrier concentration and an increase in visible light absorption. Insights from first-principles calculations relate these modifications of properties to the formation of mid-gap states localized in Cu(3d) orbitals upon oxygen vacancy formation. Furthermore, IPCE measurements rule out the possibility of successful conversion of the long wavelength light absorbed after hydrogen-treatment. Therefore, we propose the enhanced activity is due to the enhanced electron-hole pair separation kinetics, a result of higher charge carrier concentration. This study sheds light on the effect of hydrogen-treatment on the structural, optical, and electronic properties of $CuWO_4$ and the resulting improvements in PEC activity of this material.

Acknowledgments

References

1. L. Hammarstrom and S. Hammes-Schiffer, "Artificial Photosynthesis and Solar Fuels." *Accounts Chem. Res.*, **42**, 1859 (2009).
2. A. Kudo and Y. Miseki, "Heterogeneous Photocatalyst Materials for Water Splitting." *Chem. Soc. Rev.*, **38**, 253 (2009).
3. F. E. Osterloh, "Inorganic Nanostructures for Photoelectrochemical and Photocatalytic Water Splitting." *Chem. Soc. Rev.*, **42**, 2294 (2013).
4. A. Fujishima and K. Honda, "Electrochemical Photolysis of Water at a Semiconductor Electrode." *Nature*, **238**, 37 (1972).
5. A. J. Bard and M. A. Fox, "Artificial Photosynthesis - Solar Splitting of Water to Hydrogen and Oxygen." *Accounts Chem. Res.*, **28**, 141 (1995).
6. S.-R. Woo and Y.-M. Sung, "Enhanced Photoelectrochemical Water Splitting of Micro-Arc Oxidized TiO_2 via Anatase/Rutile Phase Control and Nitrogen Doping." *J. Electrochem. Soc.*, **163**, H278 (2016).
7. K. Sivula, F. Le Formal, and M. Graetzel, "Solar Water Splitting: Progress Using Hematite (alpha-Fe_2O_3) Photoelectrodes." *Chemsuschem*, **4**, 432 (2011).
8. G. Wang, Y. Ling, D. A. Wheeler, K. E. N. George, K. Horsley, C. Heske, J. Z. Zhang, and Y. Li, "Facile Synthesis of Highly Photoactive alpha-Fe_2O_3-Based Films for Water Oxidation." *Nano Lett.*, **11**, 3503 (2011).
9. F. M. Pesci, A. J. Cowan, B. D. Alexander, J. R. Durrant, and D. R. Klug, "Charge Carrier Dynamics on Mesoporous WO_3 During Water Splitting." *J. Phys. Chem. Lett.*, **2**, 1900 (2011).
10. J. Augustynski, R. Solarska, H. Hagemann, and C. Santato, "In Nanostructured Thin-Film Tungsten Trioxide Photoanodes for Solar Water and Sea-Water Splitting, Conference on Solar Hydrogen and Nanotechnology*, San Diego, CA, 2006 Aug 14–17; pp U140.
11. S. K. Arora, T. Mathew, and N. M. Batra, "Electrochemical Characteristics of Copper Tungstate Single-Crystals." *J. Phys. D Appl. Phys.*, **23**, 460 (1990).
12. G. Hitoki, T. Takata, S. Ikeda, M. Hara, J. N. Kondo, M. Kakihana, and K. Domen, "Mechano-Catalytic Overall Water Splitting on Some Mixed Oxides." *Catal. Today*, **63**, 175 (2000).
13. S. K. Arora, T. Mathew, B. Chudasama, and A. Kothari, "Single Crystal Growth and Photoelectrochemical Study of Copper Tungstate." *J. Cryst. Growth*, **275**, E651 (2005).
14. R. Lacomba-Perales, J. Ruiz-Fuertes, D. Errandonea, D. Martinez-Garcia, and A. Segura, "Optical Absorption of Divalent Metal Tungstates: Correlation between the Band-Gap Energy and the Cation Ionic Radius." *Europhys. Lett.*, **83** (2008).
15. J. E. Yourey and B. M. Bartlett, "Electrochemical Deposition and Photoelectrochemistry of $CuWO_4$, a Promising Photoanode for Water Oxidation." *J. Mater. Chem.*, **21**, 7651 (2011).

16. Y. Chang, A. Braun, A. Deangelis, J. Kaneshiro, and N. Gaillard, "Effect of Thermal Treatment on the Crystallographic, Surface Energetics, and Photoelectrochemical Properties of Reactively Cosputtered Copper Tungstate for Water Splitting." *J. Phys. Chem. C*, **115**, 25490 (2011).

17. J. C. Hill and K.-S. Choi, "Synthesis and Characterization of High Surface Area CuWO$_4$ and Bi$_2$WO$_6$ Electrodes for Use as Photoanodes for Solar Water Oxidation." *J. Mater. Chem. A*, **1**, 5006 (2013).

18. S. K. Pilli, T. G. Deutsch, T. E. Furtak, L. D. Brown, J. A. Turner, and A. M. Herring, "BiVO$_4$/CuWO$_4$ Heterojunction Photoanodes for Efficient Solar Driven Water Oxidation." *Phys. Chem. Chem. Phys.*, **15**, 3273 (2013).

19. N. Gaillard, Y. Chang, A. DeAngelis, S. Higgins, and A. Braun, "A Nanocomposite Photoelectrode Made of 2.2 eV Band Gap Copper Tungstate (CuWO$_4$) and Multi-Wall Carbon Nanotubes for Solar-Assisted Water Splitting." *Int. J. Hydrogen Energy*, **38**, 3166 (2013).

20. H. H. Chen, W. H. Leng, and Y. M. Xu, "Enhanced Visible-Light Photoactivity of CuWO$_4$ through a Surface-Deposited CuO." *J. Phys. Chem. C*, **118**, 9982 (2014).

21. K. J. Pyper, J. E. Yourey, and B. M. Bartlett, "Reactivity of CuWO$_4$ in Photoelectrochemical Water Oxidation Is Dictated by a Midgap Electronic State." *J. Phys. Chem. C*, **117**, 24726 (2013).

22. J. E. Yourey, K. J. Pyper, J. B. Kurtz, and B. M. Bartlett, "Chemical Stability of CuWO$_4$ for Photoelectrochemical Water Oxidation." *J. Phys. Chem. C*, **117**, 8708 (2013).

23. H. Zhang, P. Yilmaz, J. O. Ansari, F. F. Khan, R. Binions, S. Krause, and S. Dunn, "Incorporation of Ag Nanowires in CuWO$_4$ for Improved Visible Light-Induced Photoanode Performance." *J. Mater. Chem. A*, **3**, 9638 (2015).

24. D. Bohra and W. A. Smith, "Improved Charge Separation via Fe-Doping of Copper Tungstate Photoanodes." *Phys. Chem. Chem. Phys.*, **17**, 9857 (2015).

25. X. Chen, L. Liu, P. Y. Yu, and S. S. Mao, "Increasing Solar Absorption for Photocatalysis with Black Hydrogenated Titanium Dioxide Nanocrystals." *Science*, **331**, 746 (2011).

26. G. Wang, H. Wang, Y. Ling, Y. Tang, X. Yang, R. C. Fitzmorris, C. Wang, J. Z. Zhang, and Y. Li, "Hydrogen-Treated TiO$_2$ Nanowire Arrays for Photoelectrochemical Water Splitting." *Nano Lett.*, **11**, 3026 (2011).

27. F. M. Pesci, G. Wang, D. R. Klug, Y. Li, and A. J. Cowan, "Efficient Suppression of Electron Hole Recombination in Oxygen-Deficient Hydrogen-Treated TiO$_2$ Nanowires for Photoelectrochemical Water Splitting." *J. Phys. Chem. C*, **117**, 25837 (2013).

28. D. A. Wheeler, Y. C. Ling, R. J. Dillon, R. C. Fitzmorris, C. G. Dudzik, L. Zavodivker, T. Rajh, N. M. Dimitrijevic, G. Millhauser, C. Bardeen, Y. Li, and J. Z. Zhang, "Probing the Nature of Bandgap States in Hydrogen-Treated TiO$_2$ Nanowires." *J. Phys. Chem. C*, **117**, 26821 (2013).

29. H. S. Kim and S. H. Kang, "Effect of Hydrogen Treatment on Anatase TiO$_2$ Nanotube Arrays for Photoelectrochemical Water Splitting." *B. Kor. Chem. Soc.*, **34**, 2067 (2013).

30. S. Hoang, S. P. Berglund, N. T. Hahn, A. J. Bard, and C. B. Mullins, "Enhancing Visible Light Photo-oxidation of Water with TiO$_2$ Nanowire Arrays via Cotreatment with H$_2$ and NH$_3$: Synergistic Effects between Ti^{3+} and N." *J. Am. Chem. Soc.*, **134**, 3659 (2012).

31. M. Li, J. Deng, A. Pu, P. Zhang, H. Zhang, J. Gao, Y. Hao, J. Zhong, and X. Sun, "Hydrogen-Treated Hematite Nanostructures with Low Onset Potential for Highly Efficient Solar Water Oxidation." *J. Mater. Chem. A*, **2**, 6727 (2014).

32. J. Moir, N. Soheilnia, K. Liao, P. O'Brien, Y. Tian, K. S. Burch, and G. A. Ozin, "Activation of Ultrathin Films of Hematite for Photoelectrochemical Water Splitting via H$_2$ Treatment." *Chemsuschem*, **8**, 1557 (2015).

33. G. Wang, Y. Ling, H. Wang, X. Yang, C. Wang, J. Z. Zhang, and Y. Li, "Hydrogen-Treated WO$_3$ Nanoflakes Show Enhanced Photostability." *Energ. Environ. Sci.*, **5**, 6180 (2012).

34. G. Wang, Y. Ling, X. Lu, F. Qian, Y. Tong, J. Z. Zhang, V. Lordi, C. R. Leao, and Y. Li, "Computational and Photoelectrochemical Study of Hydrogenated Bismuth Vanadate." *J. Phys. Chem. C*, **117**, 10957 (2013).

35. A. P. Singh, N. Kodan, A. Dey, S. Krishnamurthy, and B. R. Mehta, "Improvement in the Structural, Optical, Electronic and Photoelectrochemical Properties of Hydrogen Treated Bismuth Vanadate Thin Films." *Int. J. Hydrogen Energy*, **40**, 4311 (2015).

36. M. D. Abramoff, P. J. Magalhaes, and S. J. Ram, "Image Processing with ImageJ." *Biophotonics Intern.*, **11**, 36 (2004).

37. C. D. Wagner, A. V. Naumkin, A. Kraut-Vass, J. W. Allison, C. J. Powell, and J. R. Jr. Rumble, *NIST Standard Reference Database 20*, Version 3.4 (web version) (http://srdata.nist.gov/xps/) 2003.

38. M. C. Biesinger, L. W. M. Lau, A. R. Gerson, and R. S. C. Smart, "Resolving Surface Chemical States in XPS Analysis of First Row Transition Metals, Oxides and Hydroxides: Sc, Ti, V, Cu and Zn." *Appl. Surf. Sci.*, **257**, 887 (2010).

39. S. K. Arora and T. Mathew, "Dielectric Studies of CuWO$_4$ Crystals." *Phys. Status Solidi A*, **116**, 405 (1989).